INFECTION AND IMMUNITY, Oct. 2006, p. 5549–5560 Vol. 74, No. 10
0019-9567/06/$08.00+0 doi:10.1128/IAI.00319-06

Anatomical Route of Invasion and Protective Mucosal Immunity in *Trypanosoma cruzi* Conjunctival Infection

O. K. Giddings,[1] C. S. Eickhoff,[2] T. J. Smith,[3] L. A. Bryant,[3] and D. F. Hoft[1,2]*

Department of Molecular Microbiology and Immunology,[1] Department of Internal Medicine,[2] and Department of Comparative Medicine,[3] St. Louis University Health Science Center, St. Louis, Missouri 63110

Received 24 February 2006/Returned for modification 6 April 2006/Accepted 3 July 2006

***Trypanosoma cruzi* is a protozoan parasite that can initiate mucosal infection after conjunctival exposure. The anatomical route of *T. cruzi* invasion and spread after conjunctival parasite contamination remains poorly characterized. In the present work we have identified the sites of initial invasion and replication after contaminative conjunctival challenges with *T. cruzi* metacyclic trypomastigotes using a combination of immunohistochemical and real-time PCR confirmatory techniques in 56 mice between 3 and 14 days after challenge. Our results demonstrate that the predominant route of infection involves drainage of parasites through the nasolacrimal duct into the nasal cavity. Initial parasite invasion occurs within the ductal and respiratory epithelia. After successive waves of intracellular replication and cell-to-cell spread, parasites drain via local lymphatic channels to lymph nodes and then disseminate through the blood to distant tissues. This model of conjunctival challenge was used to identify immune responses associated with protection against mucosal infection. Preceding mucosal infection induces mucosal immunity, resulting in at least 50-fold reductions in recoverable tissue parasite DNA in immune mice compared to controls 10 days after conjunctival challenge ($P < 0.05$). Antigen-specific gamma interferon production by T cells was increased at least 100-fold in cells harvested from immune mice ($P < 0.05$). Mucosal secretions containing *T. cruzi*-specific secretory immunoglobulin A harvested from immune mice were shown to protect against mucosal parasite infection ($P < 0.05$), demonstrating that mucosal antibodies can play a role in *T. cruzi* immunity. This model provides an important tool for detailed studies of mucosal immunity necessary for the development of mucosal vaccines.**

Trypanosoma cruzi is a protozoan intracellular parasite and the causative agent of Chagas disease. Approximately 16 to 18 million people in Central and South America are infected, and up to 40% will develop clinical manifestations of chronic infection (19). *T. cruzi* is transmitted by the reduviid bug when it takes a blood meal. Unlike most other insect-borne parasites, which are injected into the host while the insect feeds, the reduviid bug excretes the infective metacyclic trypomastigote in urine and feces in the process of concentrating its blood meal. Once deposited, the parasite can infect either through the wound created by the insect's bite or through mucosa after ingestion or contamination of conjunctival surfaces.

The immunopathologic manifestations of Chagas' disease develop after years of chronic infection with *T. cruzi.* These manifestations were previously thought to be due to autoimmune responses triggered by parasite epitopes cross-reactive with self-proteins. However, the development of more sensitive tools that can detect low levels of parasite persistence have implicated chronic infection and the associated parasite-specific immunity in the development of disease pathology (20). Furthermore, chemotherapeutic treatment of patients with chronic *T. cruzi* infection can lower the tissue parasite burden and protect against disease progression (5). These more recent studies indicate that vaccines capable of preventing initial *T. cruzi* infection or decreasing parasite replication in those chronically infected could be effective in preventing disease progression without triggering autoimmune pathology.

Our laboratory has previously developed a murine model of *T. cruzi* infection after oral mucosal challenge (8). It is well established that oral transmission of *T. cruzi* plays an important role in the sylvatic infection cycle, and recent descriptions of infectious outbreaks after contamination of food and beverages with *T. cruzi* insect-derived metacyclic trypomastigotes (IMT) have emphasized the importance of oral transmission in human infections (2, 3, 7, 15, 24). Our previous work showed that when mice are challenged orally with IMT, initial mucosal invasion occurs just distal to the margo plicatus, the boundary between the proximal cardiac portion of the stomach, which is lined with a stratified squamous epithelial layer, and the secretory region of the stomach, which contains the first columnar epithelium along the gastrointestinal tract. Infection via the oral route causes an increase in *T. cruzi*-specific gastric intraepithelial lymphocytes and immunoglobulin A (IgA)-secreting B cells (8). In the present study we are expanding our studies of *T. cruzi* mucosal infection and immunity to include model challenges through a second site of natural mucosal infection, the conjunctiva.

In 1935 Romaña first described the "unilateral schyzotrypanosomic conjunctivitis" associated with acute *T. cruzi* infection later known as Romaña's sign (19) and demonstrated that chronic infection and Chagas' disease could result from *T. cruzi* conjunctival inoculation. Despite the long-standing recognition of conjunctival *T. cruzi* transmission, the detailed anatomic route of invasion after conjunctival challenge has remained poorly characterized. In order to develop a model for studies of mucosal immunity, we set out to characterize the

* Corresponding author. Mailing address: Division of Infectious Diseases and Immunology, St. Louis University Health Science Center, 3635 Vista Ave., FDT-8N, St. Louis, MO 63110. Phone: (314) 577-8648. Fax: (314) 771 3816. E-mail: hoftdf@slu.edu.

initial sites of invasion and parasite replication after conjunctival challenge. We have found that after *T. cruzi* parasites are placed on the conjunctiva, they drain with tears into the nasolacrimal duct and nasal cavity, where they infect the most proximal tissues lined with cuboidal and columnar epithelial. In addition, we have shown that conjunctivally challenged mice develop type I immunity and mucosal antibody responses associated with protection against subsequent mucosal parasite challenges.

MATERIALS AND METHODS

Parasites, mice, and challenge protocol. The Tulahuèn strain of *T. cruzi* was maintained by passage through BALB/c (Harlan, Indianapolis, IN) mice and the reduviid vector *Dipetalogaster maximus*. To generate culture-derived metacyclic trypomastigotes (CMT), *T. cruzi* epimastigotes were cultured in modified Grace's medium (Sigma, St. Louis, MO) for 7 to 14 days. Parasite concentrations were determined by hemacytometer count, and the percentage of CMT was determined by DiffQuik staining (Dade International, Inc., Miami, FL). To collect IMT, *T. cruzi*-infected reduviid bugs were allowed to feed on anesthetized mice. Engorged insects were then incubated in glass vials for 3 to 4 h. Excreta from multiple reduviids were pooled, and the concentrations of IMT were determined by direct hemacytometer count. IMT preparations were concentrated by centrifugation so that 5 μl contained 200 to 1,000 parasites. Six- to eight-week-old female BALB/c mice were challenged with these CMT or IMT preparations by atraumatic deposition of 2 to 5 μl on the ocular surface of either the right eye or both eyes of anesthetized mice. All animal studies were conducted with the approval of the St. Louis University Animal Care Committee in AALAS-accredited facilities.

Preparation of histopathologic sections. Mice were sacrificed and harvested at timed intervals within 14 days of inoculation. The heads, submandibular lymph nodes, spleens, and stomachs were collected from each animal and fixed in 10% neutral buffered formalin. Intact mouse heads were decalcified overnight in RDO-rapid decalcifier (Apex Engineering Products Corp., Aurora, IL), rinsed with tap water, and returned to 10% neutral buffered formalin. Trimmed tissues were processed by gradual dehydration in graded ethanol solutions, followed by xylene immersion, and embedded in Paraplast X-tra (Oxford Labware, St. Louis, MO). Serial 5-μm tissue sections were cut, and adjacent sections were stained with hematoxylin and eosin (H&E) or by the immunohistochemical (IHC) technique described below. Stained sections were analyzed by direct light microscopy. In the most detailed experiments, slides were prepared from sections obtained every 50 μm throughout the tissue blocks.

Immunohistochemical detection of intracellular amastigotes. Serial histologic sections taken every 50 μm from formalin-fixed tissues were stained immunohistochemically to facilitate identification of *T. cruzi* intracellular amastigotes. Sections were heated at 60°C for 1 h, deparaffinized in xylene, and rehydrated with a graded series of ethanol-deionized water solutions. Tissues were stained with a polyclonal anti-CMT rabbit serum using the VECTASTAIN alkaline phosphatase ABC staining kit and visualized with VECTORED substrate (VectorLabs, Burlingame, CA). Tissues were counterstained with Hematoxylin-2 (Richard-Allan, Richland, MI). Sections taken from the spleens of uninfected control and highly parasitemic mice were included as negative and positive controls, respectively, in each experiment.

Real-time PCR detection of *T. cruzi* in conjunctiva-associated tissues. Conjunctivae, ocular tissues, lacrimal and harderian glands, parotid and submandibular lymph nodes, nasal cavities, spleens, and stomachs were harvested from mice infected by contaminative placement of differing doses of CMT or IMT on the corneal surface of anesthetized mice. DNA samples were purified by using a DNEasy kit (QIAGEN, San Diego, CA), and total DNA concentrations were adjusted to 20 to 40 ng/ml. Primers (5′-AACCACCACGACAACCACAA-3′ and 5′-TGCAGGACATCTGCACAAAGTA-3′) were used to specifically amplify a 65-bp fragment of cruzipain, with a protocol similar to one we have previously described (9). However, instead of using SYBR green detection as in our previous method, amplicon generation was detected by using a FAM/TAM probe (5′-TGCCCCAGGACCGTCCCCA-3′; Synthegen, Houston, TX) and TaqMan PCR master mix (Applied Biosystems, Foster City, CA), 900 nM concentrations of each primer, and 100 to 200 ng of sample DNA. A standard curve was generated by using positive control DNA harvested from a known concentration of *T. cruzi* epimastigotes grown in pure culture. These reactions were run in an ABI Prism 7700 sequence detector (Applied Biosystems) using the following conditions: 95°C for 10 min, followed by 40 cycles of 95°C for 15 s and 60°C for 1 min. Analysis of *T. cruzi* molecular equivalents (mEq) was performed by using sequence detection systems version 1.9a software (Applied Biosystems).

Generation of memory immune mice. Six- to eight-week-old BALB/c mice were challenged during ketamine-xylazine-induced anesthesia by contaminative placement of 200 to 1,000 *T. cruzi* IMT on bilateral ocular surfaces. These mice were rechallenged conjunctivally every 4 to 6 weeks for a total of four times over a 6-month period. At least 2 months after the final IMT challenge, the chronically infected mice were challenged with 5×10^5 CMT per eye. Three days after challenge, some of these mice were harvested for immune studies as described below. Ten days after challenge, lacrimal and harderian glands, parotid and submandibular lymph nodes, nasal cavities and nasolacrimal ducts, and spleens were harvested. To quantify parasite replication, real-time PCR was performed as described above on all tissues harvested. In addition, splenocytes and lymph node cell preparations were serially diluted and plated in 96-well microtiter plates in liver digest-neutralized tryptose broth containing 0.02 mg of hemin/ml, 100 U of penicillin/ml, 100 μg of streptomycin/ml, and 10% fetal calf serum (LDNT) as previously described (8). Plates were incubated for 2 months at 25°C and inspected every week by inverted light microscopy for outgrowth of *T. cruzi* epimastigotes. The minimal initial mononuclear cell concentrations associated with parasite outgrowth were used to estimate initial parasite concentration (reported as the number of parasites per million cells).

Assays to assess T-cell proliferation. Spleen and lymph node cells were harvested from memory immune and naive mice 3 days after parasite challenge. Total cells were plated at a concentration of 2×10^6 cells/ml in 96-well round-bottom microtiter plates. Cells were incubated with medium alone or 10 μg of *T. cruzi* lysate/ml. Plates were incubated at 37°C with 5% CO_2 for 72 h. Supernatants were then harvested, and cells were pulsed with 0.5 μCi of [^{3}H]thymidine (Amersham Biosciences Corp., Piscataway, NJ)/well. Plates were incubated for six more hours, and cells were harvested with a Tomtec Mach-IIIM cell harvester (Tomtec, Hamden, CT) onto glass filter mats. Filters were counted by using a Wallac Trilux 1450 Microbeta liquid scintillation counter (Perkin-Elmer, Boston, MA). The results are reported in disintegrations per minute.

Enzyme-linked immunospot (ELISPOT) assay to assess IFN-γ production. Millititer HA 96-well microtiter plates with nitrocellulose bases (Millipore, Bedford, MA) were coated with a monoclonal antibody specific for murine gamma interferon (IFN-γ; R46A2; American Type Culture Collection, Rockville, MD). Plates were blocked with phosphate-buffered saline (PBS) containing 10% fetal bovine serum to prevent nonspecific binding. To assess antigen specific IFN-γ secretion by both $CD4^+$ and $CD8^+$ *trans*-sialidase (TS)-specific T cells, total lymph node or spleen cells were cultured with either A20J cells in wells containing 10 μg of *T. cruzi* lysate/ml or A20J cells infected overnight with *T. cruzi* tissue culture trypomastigotes at a ratio of 20:1 (10^5 A20J with 2×10^5 mononuclear cells per well). Wells containing A20J cells alone were used as negative controls. To evaluate the relative levels of $CD8^+$ T-cell responses, a previously described H-$2k^d$-restricted epitope derived from the protective *T. cruzi* TS antigen was used to stimulate lymphocyte cultures (IYNVGQVSI) (4). A total of 2×10^5 mononuclear cells were plated per well and pulsed with 2 μM TS peptide and 30 U of interleukin-2/ml. The numbers of IFN-γ-producing cells were detected by the addition of biotinylated anti-IFN-γ (Pharmingen, San Diego, CA). Plates were developed by the addition of streptavidin conjugated to horseradish peroxidase (Jackson Immunoresearch Laboratories, West Grove, PA), followed by 3-amino-9-ethylcarbazole substrate precipitation. The results are reported as the number of spot-forming cells per million cells.

Antigen-specific IgA ELISA and IgA opsonization. *T. cruzi* specific secretory IgA (sIgA) levels were measured in tears and fecal extracts (FE) obtained from memory immune and naive BALB/c mice. Briefly, the conjunctival and ocular surfaces of five mice from each group were washed with 5 μl of PBS containing 10% fetal calf serum. These washes were pooled, and the final volume was adjusted to 50 μl. Fecal pellets were collected from five memory immune and five naive mice and pooled for each group. The pellets were dissolved in PBS containing 10% fetal bovine serum by vortexing for 15 min at room temperature. Extracts were clarified by centrifugation, and supernatants and tear preparations were serially diluted and added to Immulon II HB enzyme-linked immunosorbent assay (ELISA) plates coated with 20 μg of *T. cruzi* lysate/ml. Plates were incubated overnight at 4°C and washed with PBS–0.05% Tween 20. Biotinylated goat anti-mouse IgA (Southern Biotechnology Associates, Burlingame, AL) was added to detect bound IgA antibodies. Plates were incubated for 2 h at room temperature, washed, and developed with streptavidin conjugated to horseradish peroxidase, followed by the addition of 3,3′,5,5′-tetramethylbenzidine substrate (Sigma, St. Louis, MO). Plates were analyzed at 450 nm referenced to 540 nm. For opsonization studies, FE were passed through 0.2-μm-pore-size filters, mixed 1:1 with parasites (10^7 CMT/ml), and incubated at room temperature for 30 min. For in vitro studies, NIH 3T3 cells (American Type Culture Collection,

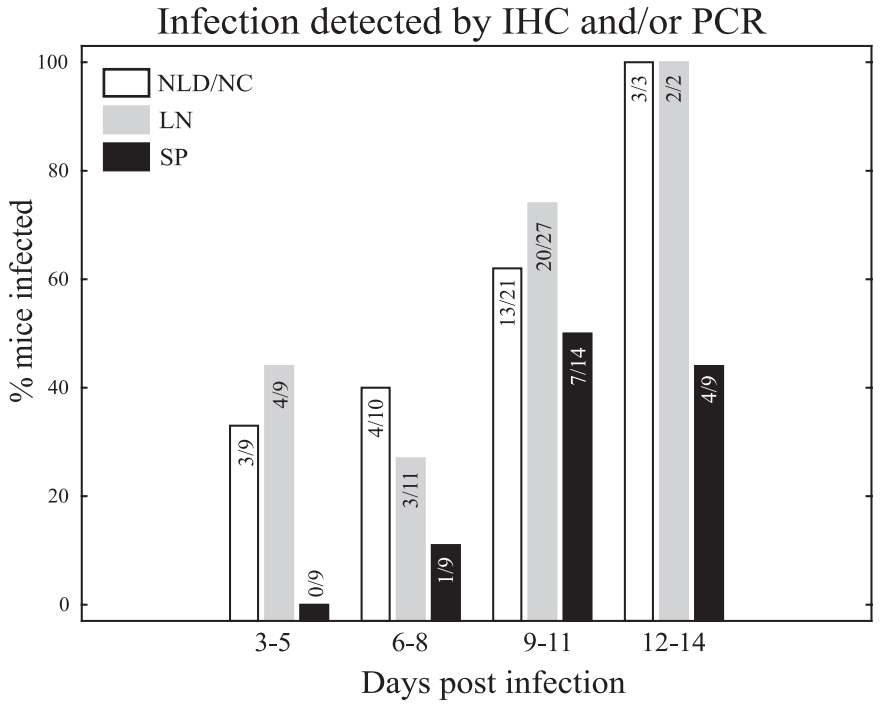

FIG. 1. *T. cruzi* first infects and replicates in local tissues, followed by systemic dissemination. A total of 56 mice were studied by immunohistochemistry and/or real-time PCR. Early after challenge (days 3 to 5) parasites were detected only in the nasolacrimal ducts and nasal cavity (NLD/NC, white bars) and draining lymph nodes (LN, gray bars). Only 9 to 11 days after infection can significant numbers of parasites be detected in more distant tissues such as the spleen (SP, black bars). The number of mice in which evidence of infection was detected is shown in the numerator of each bar while the total number of mice studied is shown in the denominator.

Manassas, VA) were plated onto eight-well chamber slides and grown to confluence. FE-opsonized CMT were diluted in PBS, and a total of 6.25×10^6 CMT were added to each well of an eight-well chamber slide. Parasites were allowed to invade for 1 h at 37°C. Slides were then washed with warm medium to remove extracellular parasites and incubated at 37°C for 48 h. Slides were then washed with PBS and stained by DiffQuik. The results are reported as the percentage of infected cells. For in vivo studies, mice were inoculated with 5 μl of each opsonized parasite suspension (containing 2×10^5 CMT) per eye as described above. Mice were sacrificed after 10 days, and DNA was isolated from the draining lymph nodes. Parasite replication was measured by real-time PCR and quantitative parasite culture as described above.

Statistics. Statistical analyses were performed with STATISTICA version 6 software (StatSoft, Inc., Tulsa, OK). Mann-Whitney U tests were used to compare responses between different groups.

RESULTS

After conjunctival challenge, *T. cruzi* undergoes replication in local tissues prior to dissemination to distant sites. In our initial studies of conjunctival infection we used IMT, the mucosally infective forms present within reduviid vector excreta, to best approximate natural infection in humans. Mice were challenged as described in Materials and Methods, with 200 to 1,000 IMT in various experiments. Additional experiments were conducted with larger doses of CMT in order to increase the sensitivity of detection. No significant differences were seen by either IHC or real-time PCR comparing infections with IMT and CMT. A total of 56 mice were studied 3 to 14 days after infection by immunohistochemistry and/or real-time PCR. To best maintain the anatomical architecture during handling for IHC studies, whole tissues were decalcified and processed for staining. For real-time PCR, DNA was extracted from fresh tissues. Our overall findings are depicted in Fig. 1. We studied nine mice between days 3 and 5 after conjunctival challenge. Of these mice, 33% showed evidence of infection in the nasal cavity and/or nasolacrimal duct, and 44% showed evidence of infection in the draining lymph nodes, while no infection was detected in the spleen. Eleven more mice were studied between days 6 and 8 after conjunctival challenge. Of these, 40, 27, and 11% showed evidence of infection in the nasolacrimal duct or nasal cavity, parotid and submandibular lymph nodes, and spleen, respectively. A total of 27 mice were studied between 9 to 11 days after challenge. Of this third group, 62, 74, and 50% showed infection in the nasolacrimal duct or nasal cavity, parotid or submandibular lymph nodes, and spleen, respectively. By 12 to 14 days after challenge, parasites were detected in the nasolacrimal duct or nasal cavity and the parotid or submandibular lymph nodes in 100% of mice, while 44% showed evidence of infection in the spleen (nine mice studied). No evidence was found in any of the mice studied by either IHC or real-time PCR to indicate infection in the conjunctiva itself, the eyelids, or the cornea (data not shown). In addition, no clinical signs of infection (e.g., palpebral edema, blepharitis, or conjunctivitis) were seen in the days after conjunctival challege. These data demonstrate that after conjunctival inoculation the predominant invasion occurs through epithelia lining the nasolacrimal ducts and nasal cavity. Parasites initially replicate within these local mucosal epithelia, spread to local lymphoid organs, and finally disseminate to distant sites. We found no evidence for parasite replication in the conjunctiva itself.

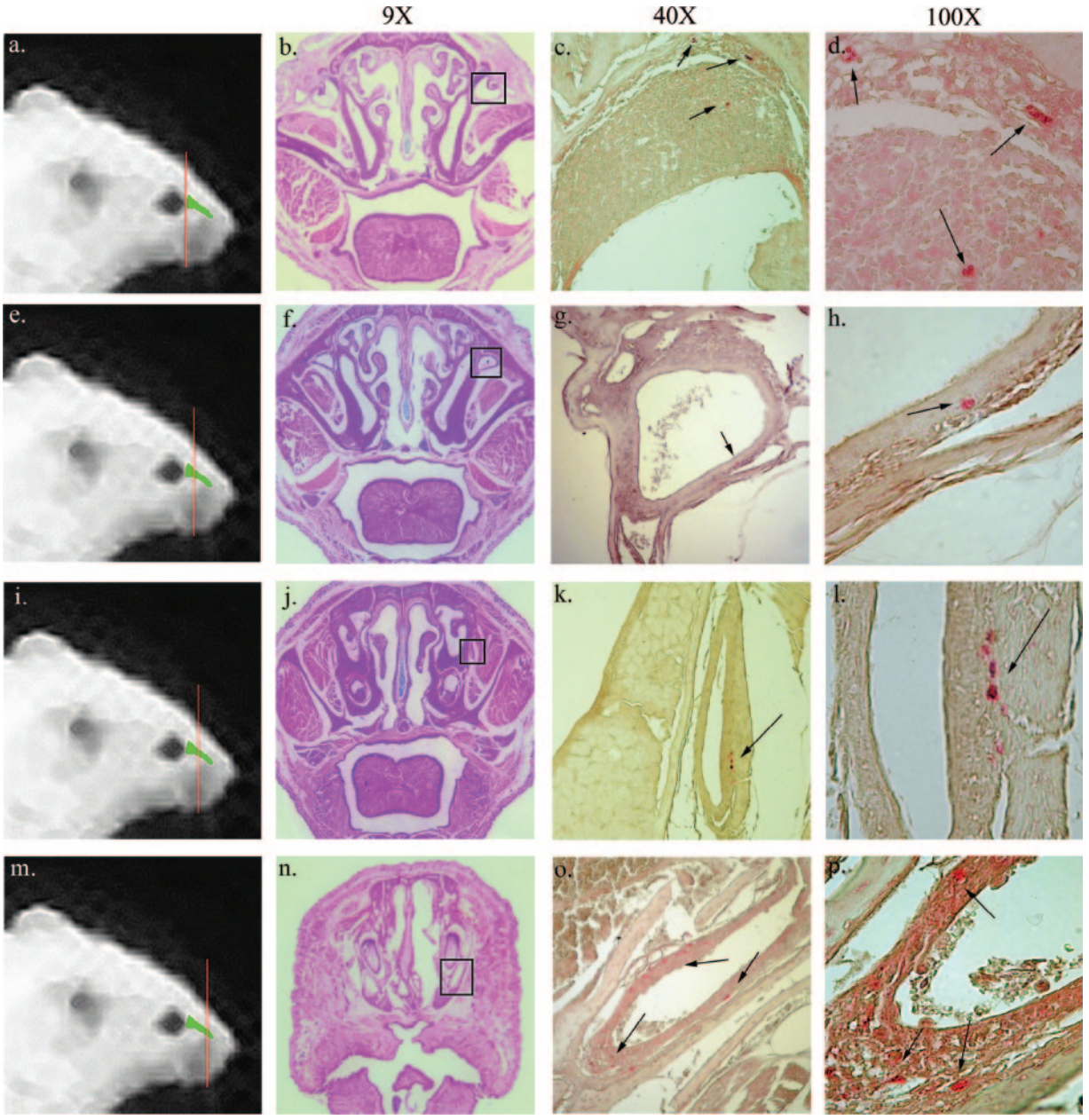

FIG. 2. *T. cruzi* infects primarily in the nasolacrimal duct after conjunctival infection. The lines drawn through the mouse heads in the first panel of each row (a, e, i, and m) indicate macroscopically the area being studied. Included are H&E-stained sections (b, f, j, and n) and *T. cruzi*-specific immunostaining (c, d, g, h, k, l, o, and p) of four different sections through the nasolacrimal duct of mice challenged conjunctivally 12 days earlier with *T. cruzi* IMT. Parasites were deposited atraumatically on the corneal surface of anesthetized mice. The H&E-stained sections show a low-power (×9 magnification) view of the section to orient the reader (b, f, j, and n). The boxed areas in the H&E views identify the regions studied in adjacent sections by immunohistochemistry and shown at higher power to the right. Panels c, f, k, and o show parasite-specific immunohistochemical staining (×40 magnification). Panels d, h, l, and p show the same sections at ×100 magnification. Intracellular amastigotes stain brightly red-orange by immunohistochemistry. These results indicate infection and parasite replication along the length of the nasolacrimal duct.

Further evidence that epithelia lining the nasolacrimal ducts and nasal cavities are the predominant sites of invasion after *T. cruzi* conjunctival challenge. To further define in detail the anatomical route of infection after conjunctival challenge, we performed extensive IHC studies of serial sections from the heads of eight conjunctivally challenged mice. Intracellular amastigotes were seen within epithelia lining the nasolacrimal ducts in seven of eight infected mice (Fig. 2.). Parasite pseudocysts were found as early as 8 days after challenge in the lacrimal sac at the proximal end of the nasolacrimal duct draining tears from the eye (Fig. 2a to d) and at later time points through the length of the duct (Fig. 2e to l) to its distal end, where it drains into the nasal cavity (Fig. 2m to p). This is the most proximal tissue in which parasites were seen, as well as

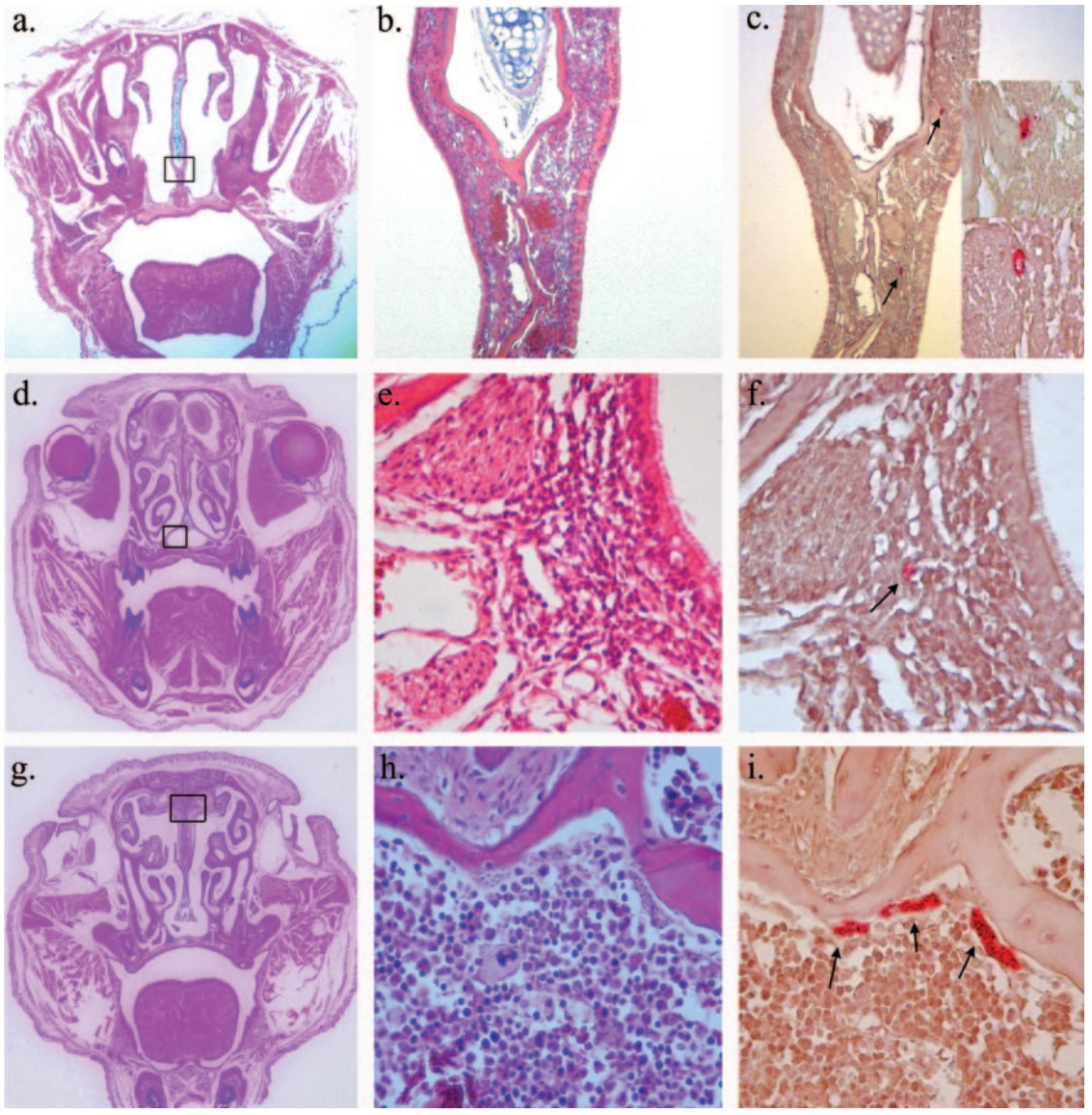

FIG. 3. *T. cruzi* infects the nasal cavity and lacrimal gland. In each row the first panel (a, d, g, and j) presents a low-power view (×9 magnification) of the entire section being studied to orient the reader. All panels in the first row (a, b, c, and c inset) show parasite pseudocysts in the subepithelial layer of the nasal septum (panels b and c are shown at ×40 magnification, while the panel c inset shows the same at higher magnification [×100 magnification]). The panels in the second row (panels d, e, and f) show infection within a specialized inductive lymphoid tissue found within the nasal cavity (nasal mucosa-associated lymphoid tissue) (panels e and f are at ×100 magnification). The panels in the third row (panels g, h, and i) show infection within the bone marrow of the nasal septum (panels h and i are both shown at ×100 magnification).

the first nonstratified squamous epithelia the parasite contacts after conjunctival inoculation.

We also found consistent evidence for infection within the epithelia lining the nasal cavity. Intracellular amastigotes were seen in this area in five of eight mice studied by IHC. Parasites were seen in a number of different areas adjacent to the nasal cavity, including the submucosa of the epithelial lining of the nasal septum (3a to c), the nasal mucosa-associated lymphoid tissue, an inductive lymphoid organ analogous to the tonsils and adenoids in humans (Fig. 3d to f), and in the bone marrow of the facial bones surrounding the nasal cavity (Fig. 3g to i). We also saw occasional infection in the lacrimal and harderian glands (data not shown). No evidence of infection was found in the eyelid, conjunctiva, orbit, or any other facial tissues excluding the lacrimal system and nasal cavity. These data suggest *T. cruzi* infects the first nonstratified squamous epithelia it contacts and undergoes multiple rounds of intracellular replication and local spread.

Local parasite spread is lateralized to the side of conjunctival challenge. In our initial IHC experiments we challenged mice by placing parasites on the surface of the right conjunctiva only. We hypothesized that initial local spread of infection would be limited to the side of challenge, whereas rapid systemic spread would result in bilateral evidence of infection. We harvested lymph nodes from both the challenged and unchallenged sides and compared the results. At the time of harvest

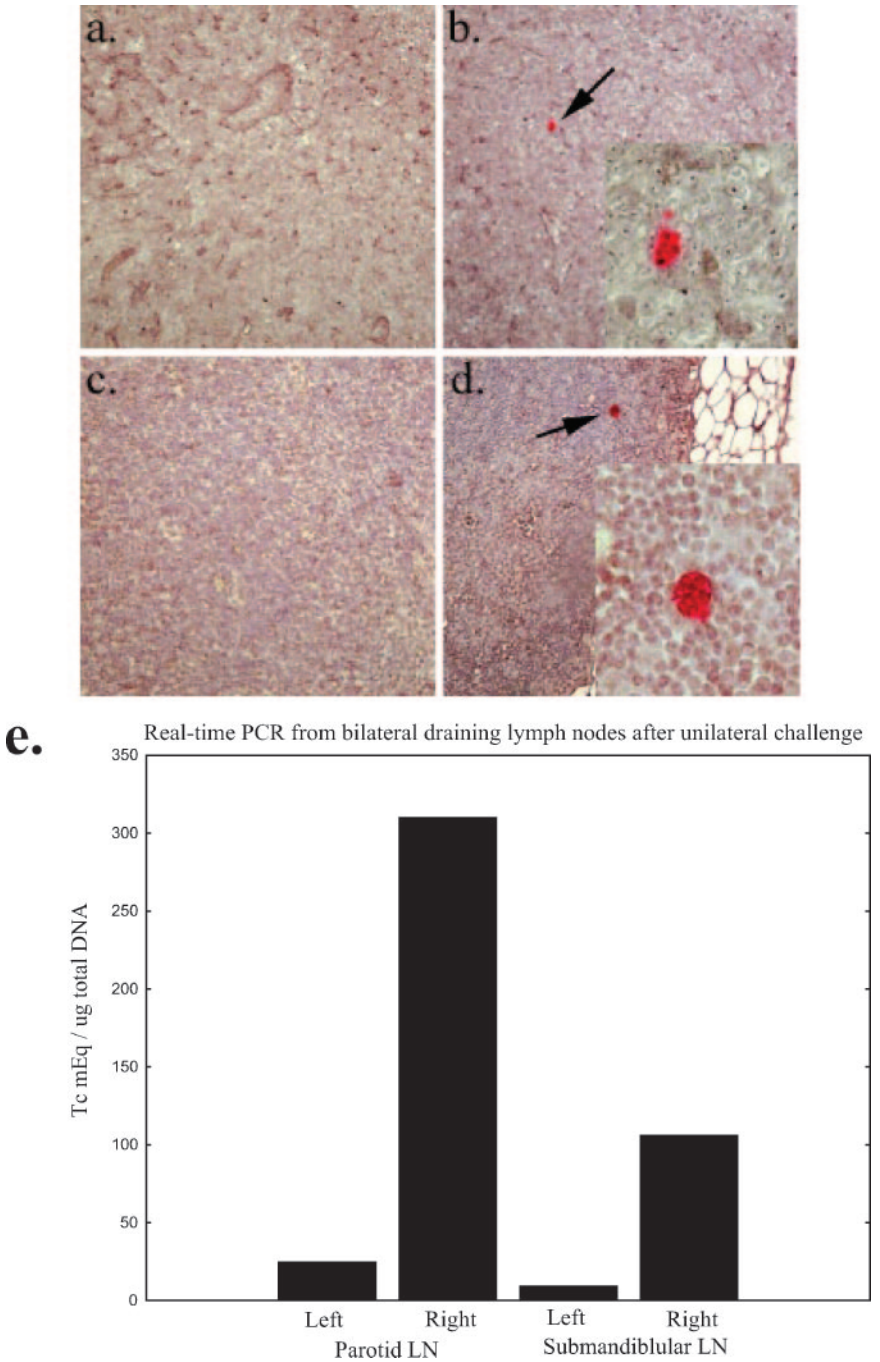

FIG. 4. *T. cruzi* infection is limited to the ipsilateral side of challenge. (a to d) IHC staining of the right and left submandibular lymph nodes harvested from two separate mice 12 days after infection by contaminative challenge of the right eye. The left submandibular lymph nodes (a and c) show no signs of intracellular amastigotes, the replicative form of the parasite. In contrast, *T. cruzi* pseudocysts can be detected by immunohistochemistry in the right lymph nodes (b, b inset, d, and d inset). Proliferative centers were also seen in the right but not left lymph nodes (data not shown). (e) Further evidence for lateralization of infection by real-time PCR. Mice were infected by contaminative challenge of the right eye in the manner described above. The left eyes were exposed to an inactivated *T. cruzi* whole lysate prepared from numbers of parasites similar to those used for live challenge, and 10 days after infection the submandibular and parotid lymph nodes were harvested for DNA extractions. Real-time PCR was performed as described in Materials and Methods. Significant levels of parasites were seen in the right lymph nodes but not in the left.

we noted that the draining lymph nodes from the challenged side were enlarged compared with the nonchallenged side (results not shown). We sectioned completely through the bilateral lymph nodes of several mice, staining sections every 50 μm. Evidence for infection during the first 2 weeks after challenge was found only in the draining lymph nodes ipsilateral to the live parasite challenge (Fig. 4a to d). To confirm these findings and prove that our real-time PCR assay detected par-

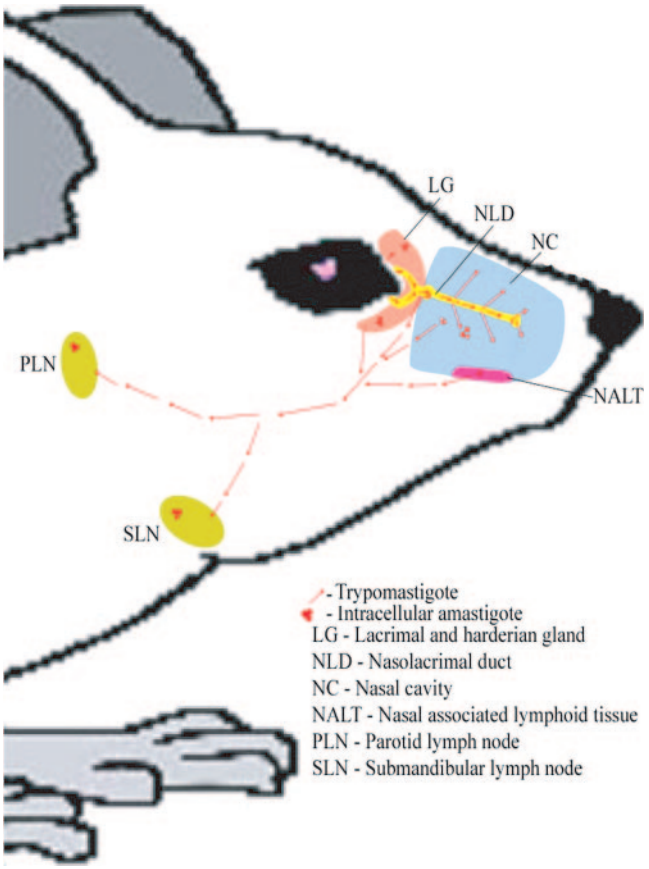

FIG. 5. *T. cruzi* infects and replicates in the nasolacrimal duct and nasal cavity after conjunctival challenge. The conjunctiva is exposed to trypomastigotes from the insect vector (red arrows). This form of the parasite gains access to the nasolacrimal duct with normal tear drainage or to the lacrimal gland (likely through the lacrimal secretory ducts). In these tissues the parasite can invade the transitional or cuboidal epithelium and differentiate into the intracellular amastigote (red clusters). After replication, the parasite differentiates into the blood-form trypomastigotes (red arrows), lyses the host cell, and can then infect neighboring cells or spread to other tissues through blood and lymph. Parasites eventually disseminate through the blood to distant tissues.

asite replication and not merely the parasite input from the challenge, we exposed a group of mice to live parasites on the right conjunctivae and freeze-thawed parasites on the left conjunctivae. The draining lymph nodes were harvested 10 days after challenge for DNA extraction. Real-time PCR results from these mice are shown in Fig. 4e. These data confirm the lateralization seen in our IHC studies and confirm that our PCR assay is detecting only replicating parasites. Our combined data delineate the anatomical course of infection after *T. cruzi* conjunctival inoculation as depicted in Fig. 5. Trypomastigotes (red arrows) usually drain from the conjunctivae through the nasolacrimal ducts and into the nasal cavities. Within the nasolacrimal ducts and nasal cavity, parasites infect the superficial columnar epithelia, differentiate into amastigotes, and replicate intracellularly (Fig. 5, red clusters). Trypomastigotes released from these infected cells can then continue to spread locally and eventually reach the draining lymph nodes and spread systemically through the blood and lymph. Occasionally, trypomastigotes can swim upstream from the conjunctival surface through the secretory ducts of the lacrimal and harderian glands, initiating local infection through the epithelia lining these structures.

Natural *T. cruzi* infection induces mucosal immunity that is protective against subsequent conjunctival challenge. To study the importance of mucosal immunity for protection against *T. cruzi* conjunctival challenge, we used a memory-immune model induced by natural infection. BALB/c mice were challenged conjunctivally with IMT or CMT several times over a 6-month period. Multiple challenges ensured that the mice became infected with *T. cruzi* and that potent parasite-specific immune responses were boosted by the subsequent challenges. Three months after the last conjunctival challenge, mice were inoculated with a subcutaneous dose of 5×10^3 *T. cruzi* blood form trypomastigotes (BFT), a lethal dose in naive BALB/c mice. This was done to confirm that our mice had previously developed chronic *T. cruzi* infection associated with concomitant protective immunity (mice not previously infected do not survive this BFT challenge). One month later, these chronically infected mice were challenged conjunctivally with 10^6 CMT bilaterally, in parallel with naive control mice. Ten days after challenge, the mice were sacrificed and the nasal cavities (combined with the associated nasolacrimal ducts), lacrimal and harderian glands, parotid and submandibular lymph nodes, and spleens were harvested. DNA was isolated, and real-time PCR assays were performed on all tissues. In addition, viable parasites present in spleen and lymph node cell preparations were quantified by limiting dilution cultures as described in Materials and Methods. In all comparisons, tissues from nonimmune control mice contained significantly higher levels of tissue parasitism. Means of 1,200 to 6,400 *T. cruzi* mEq per μg of total DNA were detected in all tissues harvested from conjunctivally infected nonimmune mice compared to virtually undetectable levels (means of 0 to 100 *T. cruzi* mEq per μg of total DNA) present in tissues harvested from the chronically infected memory-immune mice (Fig. 6a). All comparisons demonstrated at least 50-fold increases in the amount of parasite DNA detected in control compared to memory-immune mice. Similar differences were seen in parasite outgrowth cultures assaying for numbers of live parasites (Fig. 6b). The recovery of live parasites was 5- to 20-fold greater from nonimmune controls compared to memory-immune mice. All of these differences between memory-immune and control mice were statistically significant as determined by Mann-Whitney U tests ($P < 0.02$ and $P < 0.04$ for PCR and parasite outgrowth studies, respectively; $n = 5$/group).

Immune studies of protective mucosal responses induced by natural *T. cruzi* infection. We next wanted to identify the components of the immune response associated with mucosal protection against *T. cruzi* conjunctival challenge. BALB/c mice were conjunctivally challenged four times over a 6-month period with 200 to 1,000 IMT. At least 2 months after the final infection, these chronically infected memory-immune mice and naive controls were challenged with 5×10^5 CMT bilaterally. Three days after challenge the mice were sacrificed, and draining parotid and submandibular lymph nodes, as well as spleens, were harvested for immune studies. Lymph node and spleen cell preparations were cultured for 72 h with either medium alone or whole parasite lysate and studied for lymphoprolif-

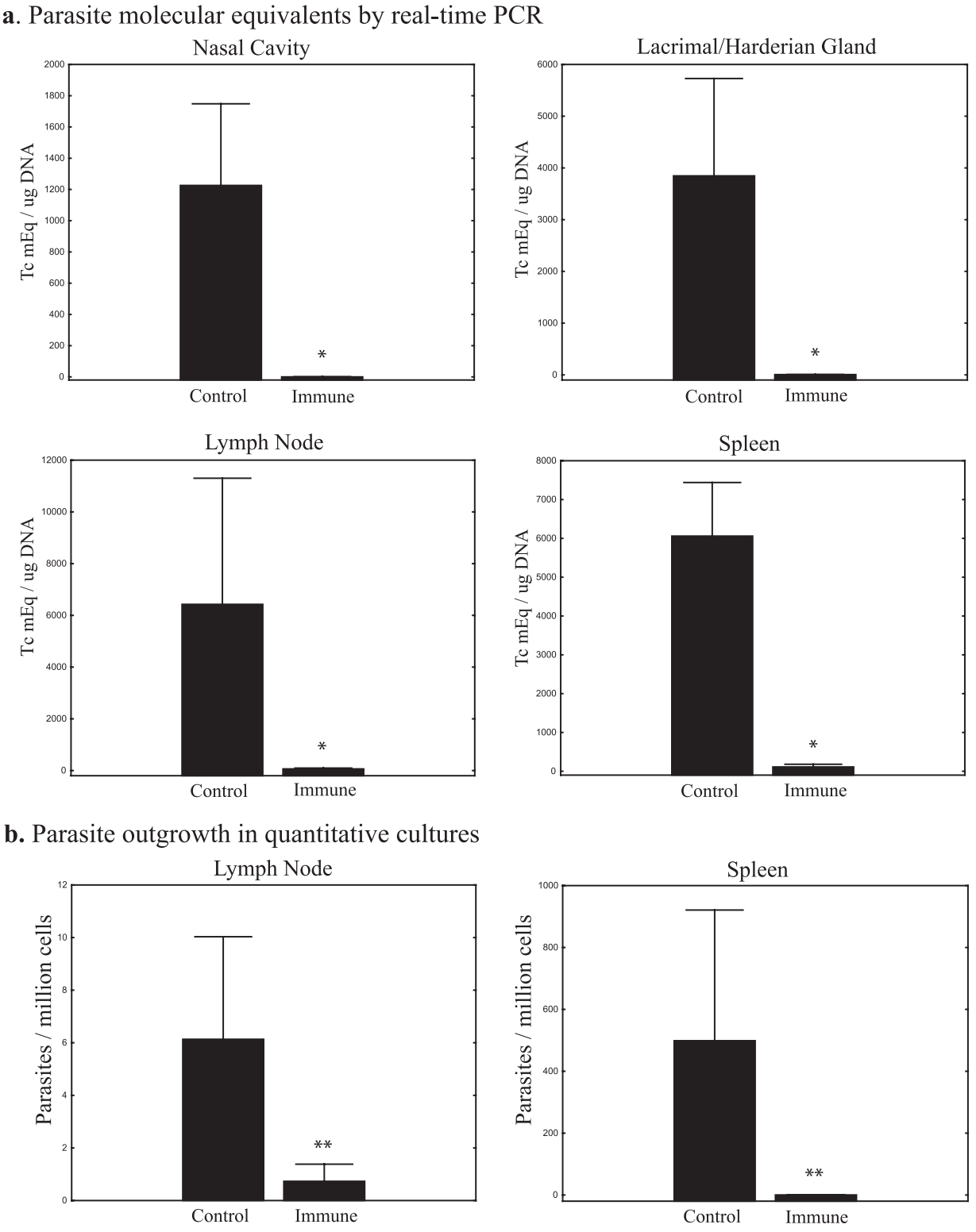

FIG. 6. Immune mice are protected against subsequent conjunctival challenge. Levels of infection in both memory immune and control mice were measured by real-time PCR and quantitative parasite culture 10 days after conjunctival challenge with 10^6 CMT. In panel a, the numbers of *T. cruzi* molecular equivalents per microgram of total DNA are shown for the nasal cavity (including the nasolacrimal duct), the lacrimal and harderian glands, the parotid and submandibular lymph nodes, and the spleen (*, $P < 0.02$ [Mann-Whitney U test]; $n = 5$). In panel b, parasite outgrowths from mononuclear cell preparations are shown for draining lymph nodes and spleen (**, $P < 0.04$ [Mann-Whitney U test]; $n = 5$). In both panels vertical bars represent the standard errors of the means.

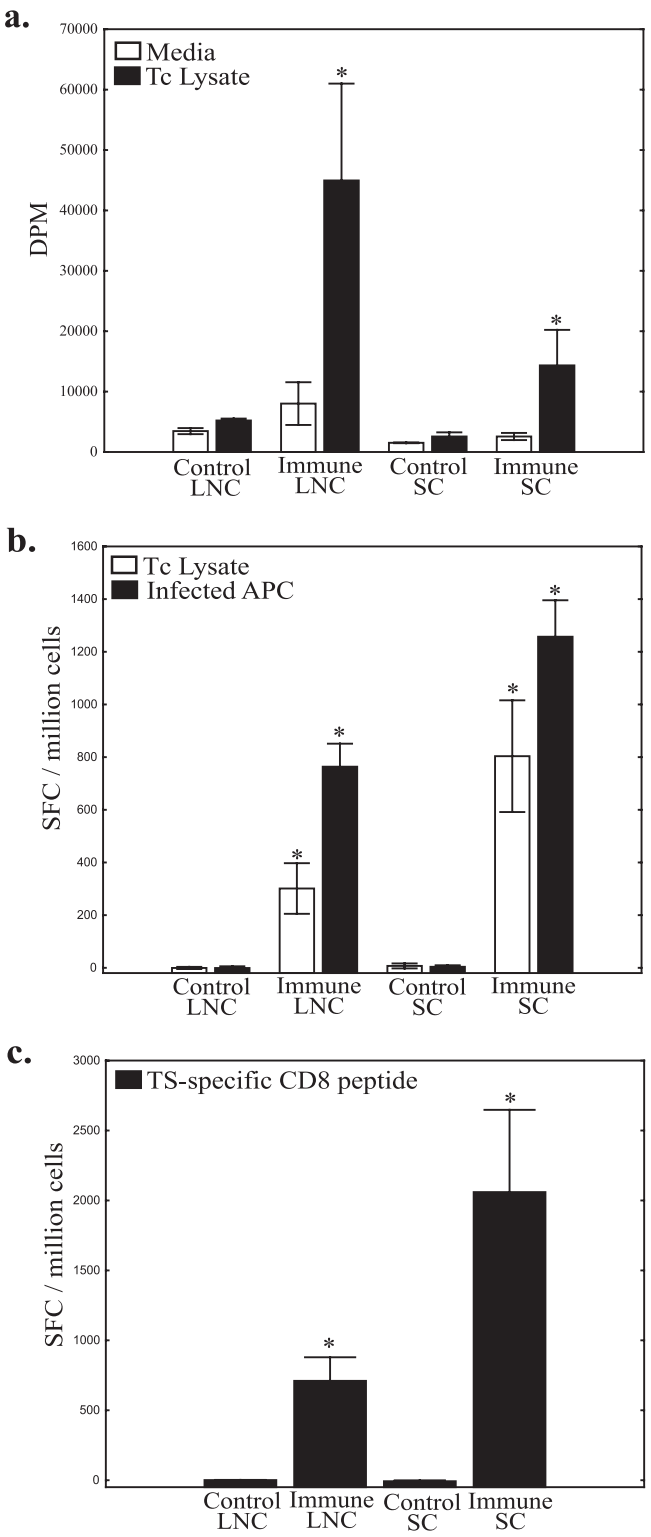

FIG. 7. Lymph node and spleen cells from immune mice proliferate and produce significant levels of IFN-γ in response to antigen. (a) Both lymph node cells and spleen cells from memory immune mice challenged 3 days previously display significantly increased lymphoproliferation in response to whole parasite lysate (*, $P < 0.05$ [Mann-Whitney U test]). (b) The same trend is seen in the IFN-γ ELISPOT assay. Increased numbers of memory-immune lymph node cells and spleen cells secrete IFN-γ when cocultured with whole parasite lysate (□) or A20J cells infected with *T. cruzi* (■) (*, $P < 0.03$ [Mann-Whitney U test]). (c) Memory-immune lymph node and spleen cells incubated with a *T. cruzi* TS-specific CD8 epitope produced significantly increased numbers of IFN-γ-secreting cells (*, $P < 0.05$ [Mann-Whitney U test]). In all panels, vertical bars represent the standard errors of the means. SFC, spot-forming cells.

erative responses by thymidine incorporation as described in Materials and Methods (Fig. 7a). The proliferative responses of lymph node cells stimulated with parasite lysate were increased more than eightfold in memory-immune mice compared to infected controls. Splenic lymphoproliferative responses were more than fivefold greater in the memory-immune mice. The memory-immune responses were significantly increased compared to controls ($P < 0.05$ [Mann-Whitney U test], $n = 3$/group).

To further study parasite-specific effector immune responses, we performed IFN-γ ELISPOT assays as described in Materials and Methods. Different aliquots of the cell preparations described above were cocultured with negative control A20J cells, A20J cells pulsed with *T. cruzi* lysate, or A20J cells infected with live *T. cruzi* trypomastigotes. Parasite lysate induced more than 100- and 150-fold-higher numbers of cells to produce IFN-γ in memory-immune lymph node and spleen cell cultures, respectively (Fig. 7b). *T. cruzi*-infected A20J cells induced 200- and 250-fold increases in the numbers of cells producing IFN-γ in memory-immune lymph node and spleen cells, respectively (Fig. 7b). Similar increases in memory-immune secreted IFN-γ responses were seen by ELISA (results not shown). To examine $CD8^+$ T-cell responses, we cultured lymphocyte preparations with the previously identified TS-specific, $CD8^+$ T-cell epitope restricted to H-$2k^d$ (peptide IYNV GQVSI) (4). TS peptide stimulation induced 700- and 2,000-fold increases in the number of IFN-γ-producing cells in memory-immune lymph node and spleen cell cultures, respectively (Fig. 7c). These increases in memory-immune IFN-γ responses were significantly different from control responses ($P < 0.05$ [Mann-Whitney U test], $n = 3$/group). These data indicate that potent type I immune responses in the lymph nodes draining the sites of mucosal invasion and spleen were associated with mucosal protection against *T. cruzi* conjunctival challenge.

Conjunctival infection with *T. cruzi* stimulates sIgA responses associated with protection. Pathogen-specific sIgA is known to play an important role in protective mucosal immune responses. To assay for this marker of mucosal immunity, tears and fecal extracts were harvested from memory-immune and naive control mice. The levels of *T. cruzi*-specific sIgA present in both tears and fecal extracts were assessed by ELISA as described in Materials and Methods (Fig. 8a and b). These data indicate that conjunctivally infected mice develop marked increases in *T. cruzi*-specific mucosal immune responses compared to naive controls both at the site of challenge and in other mucosal tissues.

To assess the ability of *T. cruzi*-specific mucosal antibody to inhibit parasite infection in vitro, we opsonized CMT preparations with FE from memory-immune mice or naive control mice as described in Materials and Methods. FE were used instead of tears because the volume of tears that could be

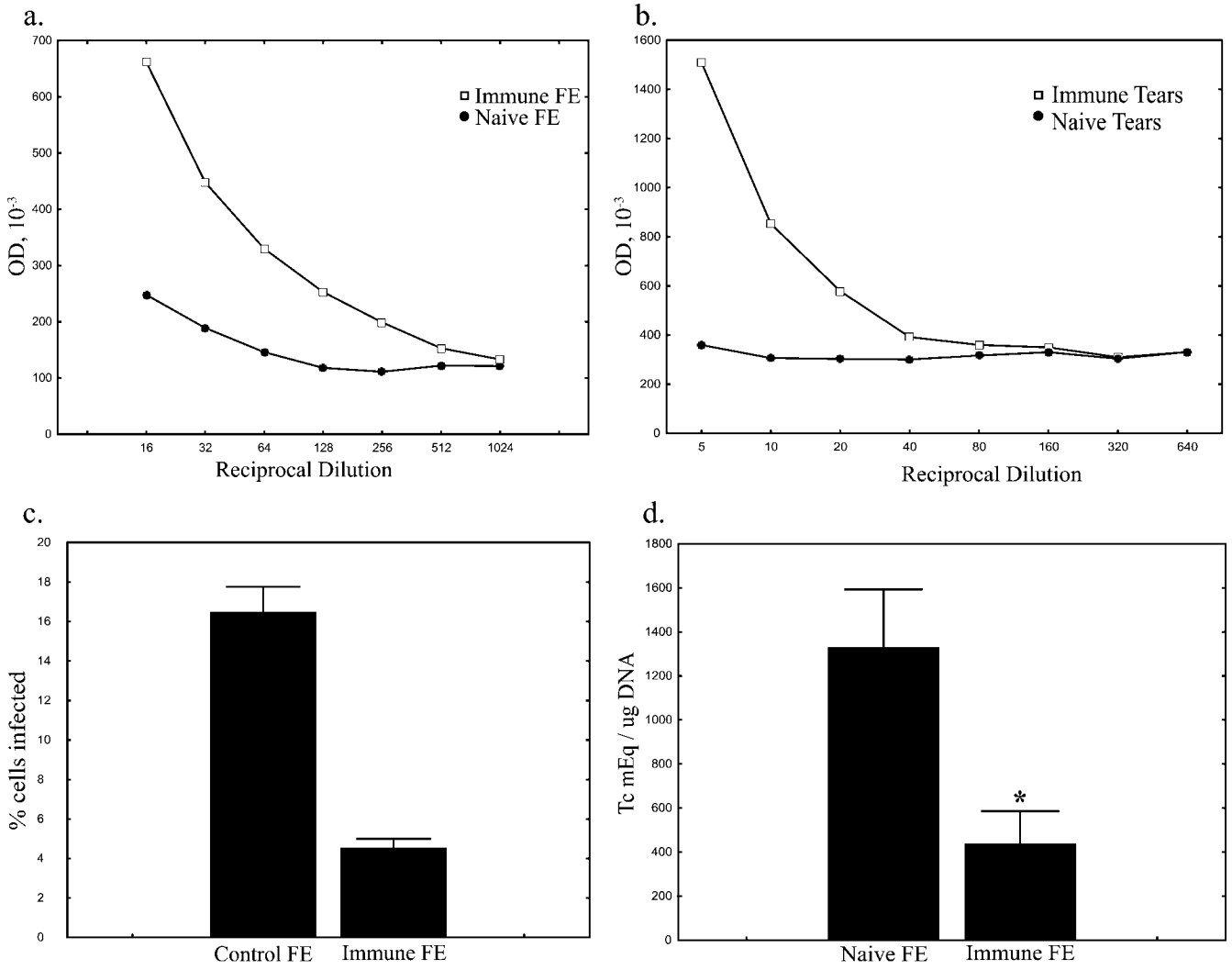

FIG. 8. Immune mice produce protective sIgA. FE and tears from memory-immune mice contain high levels of *T. cruzi*-specific IgA. FE (a) and tears (b) were harvested from five memory-immune mice and five naive control mice and pooled. The levels of *T. cruzi*-specific sIgA were assayed by ELISA. Plates were coated with whole *T. cruzi* lysate and incubated with serially diluted FE and tear samples as described in Materials and Methods. (c) Opsonization with *T. cruzi*-specific sIgA inhibits infection of NIH 3T3 cells in vitro. Parasites were opsonized with FE from memory-immune and control mice for 30 min, incubated with monolayers of 3T3 cells in eight-well chamber slides, and Giemsa stained 48 h later. (d) Opsonization with *T. cruzi*-specific sIgA inhibits infection after conjunctival challenge. Parasites were opsonized with filtered FE from memory-immune or naive control mice for 30 min. Naive BALB/c mice were challenged with opsonized parasite suspensions as described in Materials and Methods. At 10 days after challenge, DNA was isolated from the draining lymph nodes, and the parasite levels were assayed by real-time PCR. Parasites opsonized with FE from memory-immune mice resulted in significantly lower levels of infection than those opsonized with FE from control mice (*, $P < 0.05$ [Mann-Whitney U test]; $n = 6$ and 7 in memory-immune and control groups, respectively).

collected was limited. Briefly, opsonized CMT were incubated with confluent NIH 3T3 cells in eight-well chamber slides for 1 h, and then extracellular parasites were washed away with warm medium. After 48 h the slides were washed with PBS and stained with DiffQuik. Slides were examined by light microscopy, and the percentage of infected cells was determined. Wells infected with naive FE-opsonized parasites were associated with fourfold-higher levels of percent infected cells compared to those infected with CMT opsonized with *T. cruzi*-specific mucosal antibody (Fig. 8c). The number of amastigotes per infected cell was also determined (data not shown) and was not significantly different between the two groups. These data suggest that opsonization with parasite-specific mucosal antibodies can inhibit parasite invasion but does not significantly affect parasite replication once cellular infection has been established.

To determine whether *T. cruzi*-specific mucosal antibody protects against parasite challenge, we opsonized CMT with FE from memory-immune or naive mice for 30 min at room temperature prior to challenge. At 10 days after challenge the mice were sacrificed, and DNA was isolated from the draining lymph nodes. The parasite levels were assayed by real-time PCR. Significantly decreased levels of tissue parasitism were seen in mice challenged with CMT opsonized with FE containing *T. cruzi*-specific mucosal antibodies (Fig. 8d). Similar decreases in the recovery of viable parasites from these mice were

seen by quantitative culture techniques (data not shown). These results demonstrate that *T. cruzi*-specific mucosal antibody responses can decrease parasite invasion at the initial sites of mucosal infection.

DISCUSSION

We describe here the anatomical route of parasite invasion after conjunctival challenge and immune responses associated with protection against infection via this route. Our data have shown that the parasite does not directly infect the conjunctiva but first infects the epithelia lining the nasolacrimal ducts and nasal cavities. After several rounds of replication, parasites spread through local tissues, eventually reaching the draining parotid and submandibular lymph nodes. The parasite can then disseminate to distant tissues via blood and lymph. In addition, we have demonstrated by both real-time PCR and parasite outgrowth that mice chronically infected with *T. cruzi* develop immunity capable of preventing local tissue parasitism after subsequent challenges. These latter results suggest that it may be possible to generate vaccines protective against mucosal *T. cruzi* infection. Studies of infection with a number of intracellular pathogens indicate that type I immune responses are essential for the control of intracellular parasites (1, 9–12, 18, 21, 22). In addition, we have shown previously that type I immune responses are critical for mucosal protection after *T. cruzi* oral challenges (9, 12). We now demonstrate that type I T-cell responses (associated with antigen-specific lymphoproliferation, IFN-γ production, and $CD8^+$ T-cell responses) are associated with the inhibition of mucosal intracellular *T. cruzi* replication after conjunctival challenge. In addition to these markers of type I immunity, we also have shown that *T. cruzi*-specific mucosal antibodies are associated with a protective immune response and that opsonization of parasites with *T. cruzi*-specific mucosal antibody can protect against mucosal infection.

In our previous study of *T. cruzi* mucosal infection and immunity after oral parasite challenge (8), we demonstrated that the parasite infects through the proximal gastric epithelium just distal to the margo plicatus, the junction between the cardiac and glandular regions of the stomach. This point of initial invasion after oral *T. cruzi* challenge contains the first example of a simple columnar epithelium the parasite encounters after being swallowed. We now present analogous findings after conjunctival *T. cruzi* inoculation. No evidence for invasion through either the conjunctiva or cornea, which are both lined with stratified squamous epithelia, was detected. However, parasite infection was seen in the proximal nasolacrimal duct, the first nonsquamous epithelium that the parasite contacts. We hypothesize that this pattern of infection is related to the likely fact that the more proximal stratified squamous epithelia present within the gastrointestinal tract, cornea, and conjunctiva cannot support productive *T. cruzi* infection and/or replication. *T. cruzi* infection of nonphagocytic cells is an active process by both parasite and host cells (25). Parasite attachment triggers Ca^{2+} signaling within the host target cell, recruitment of endosomes to the cell membrane adjacent to the site of parasite attachment, and active phagocytic engulfment of the invading parasite. The cells in the superficial layers of stratified squamous epithelia are dead and probably cannot participate in these cellular signaling mechanisms required for *T. cruzi* intracellular invasion (26).

Both of our models of mucosal *T. cruzi* infection were developed in BALB/c mice (8). Although the mouse is a very useful model for research, murine infection is not identical to human infection. There are some differences between conjunctival infection in mice and humans, most notably the absence of Romaña sign in mice (the unilateral periorbital swelling often seen during the acute phase of Chagas' disease in humans after conjunctival transmission). The lack of palpebral edema after murine conjunctival challenge is likely due to differences in the anatomy of humans compared to mice. The lacrimal gland in the mouse is retro-orbital, whereas in humans it is supraorbital, allowing for the appearance of swelling during inflammatory processes. Furthermore, the periorbital connective tissues in humans are less dense than in mice, allowing for more swelling and edema. Despite these differences the predominant anatomical sites of parasite invasion and replication after conjunctival inoculation are likely to be similar in humans and mice. We presume that *T. cruzi* trypomastigotes drain into the nasolacrimal ducts and nasal cavities of humans, initiating infection in these epithelial surfaces as we have shown in mice.

We demonstrate here, as have previous studies in a variety of challenge models (9, 10, 12), that mice chronically infected with *T. cruzi* are resistant to subsequent infection. In fact, splenocytes from these chronically infected mice are capable of conferring protective immunity to both naive and SCID mice after adoptive transfer (10). The detailed components of immunity necessary for the prevention of infection after conjunctival or other mucosal exposures remain to be elucidated. We hypothesize that mucosal protection requires the induction of Th1 type $CD4^+$ T-cell responses, as well as cytolytic T-cell responses. In addition, it is likely that sIgA is important for protection against the initial mucosal invasion and subsequent rounds of parasite replication. We have previously shown that vaccinations inducing Th1 responses are associated with optimal mucosal protection against *T. cruzi* oral challenge and are associated with potent sIgA responses (8, 12). In the present study we have further shown that Th1 and Tc1 responses are associated with protection against conjunctival mucosal *T. cruzi* challenges.

The results shown in Fig. 8 provide the first direct evidence for protective effects of sIgA against *T. cruzi.* We have previously demonstrated, and now confirm, that parasite-specific mucosal antibodies are associated with protection against mucosal infection with *T. cruzi.* In the present study we show in both in vitro and in vivo systems that *T. cruzi*-specific mucosal antibodies inhibit infection. Our in vitro assay demonstrates that opsonization with mucosal antibodies of parasites prior to incubation with cell monolayers decreases invasion of the host cell but does not affect the ability of the parasite to replicate once infection is established. Our in vivo data indicate that opsonization with parasite-specific mucosal antibodies provides significant protection against conjunctival *T. cruzi* challenge. Possible targets of protective mucosal antibodies include but are not limited to TS, gp82, and cruzipain, all molecules that are known to be involved in infection of the mammalian host. The results of our opsonization and immune studies suggest that the development of a vaccine to prevent *T. cruzi*

infection may be a reasonable goal and that the induction of sIgA should be included in the vaccine strategy.

There are a number of *T. cruzi* antigens that are candidates for vaccine development (6, 9, 10, 12–14, 16, 17, 21, 23, 27–29). Our laboratory has worked extensively with cruzipain and TS in Th1 biasing vaccination protocols. Both of these antigens have been shown to induce protection against lethal *T. cruzi* challenges in naturally susceptible BALB/c mice (9, 10, 12, 21). In addition, opsonization of *T. cruzi* with a monoclonal antibody against gp82 has been shown to inhibit invasion of the parasite after oral challenge (17). Asp-2 has been used in combination with TS to protect naturally susceptible mice (27). These studies support the rationale for the development of preventative and therapeutic vaccines for Chagas' disease. Our murine models of *T. cruzi* mucosal infection can be used to assess the capacity of experimental vaccines to protect against oral and conjunctival parasite exposures.

T. cruzi is only one example of a group of pathogens capable of infecting their hosts through mucosal surfaces and causing significant chronic pathology. Other examples include *Mycobacterium tuberculosis*, as well as the human immunodeficiency virus, human papilloma virus, the protozoan parasite *Toxoplasma gondii*, and many others. The existence of a network known as the common mucosal immune system (CMIS) suggests that advances in the understanding of immunity directed against *T. cruzi* conjunctival infection may apply to infection with other mucosal pathogens. Currently, the majority of research investigating the CMIS has focused on studies of the small intestine. By developing additional models to study other mucosal inductive and effector immune tissue sites, we have provided valuable tools for the study of the CMIS. *T. cruzi* is an ideal pathogen for these studies because it is capable of infecting through multiple mucosal and systemic routes naturally during the normal transmission of the parasite. With our models of different mucosal infections we are well equipped to study in detail the differential requirements of memory immune trafficking to different mucosal and systemic tissues. Further studies could lead to effective mucosal vaccine protocols for the prevention of *T. cruzi* infection and disease specifically and mucosal pathogens in general.

REFERENCES

1. **Abbas, A. K., K. M. Murphy, and A. Sher.** 1996. Functional diversity of helper T lymphocytes. Nature **383:**787–793.
2. **Bittencourt, A. L., M. Sadigursky, A. A. Silva, C. A. S. Menezes, M. M. M. Marianetti, S. C. Guerra, and I. Sherlock.** 1988. Evaluation of Chagas' disease transmission through breast-feeding. Mem. Inst. Oswaldo Cruz. **83:** 37–39.
3. **Calvo Mendez, M. L., B. Nogueda Torres, and R. Alejandre Aguilar.** 1992. La via oral: una puerta de acceso para *Trypanosoma cruzi*. Rev. Latinoam. Microbiol. **34:**39–42.
4. **Fujimura, A. E., S. S. Kinoshita, V. L. Pereira-Chioccola, and M. M. Rodrigues.** 2001. DNA sequences encoding $CD4^+$ and $CD8^+$ T-cell epitopes are important for efficient protective immunity induced by DNA vaccination with a *Trypanosoma cruzi* gene. Infect. Immun. **69:**5477–5486.
5. **Garcia, S., C. O. Ramos, J. F. Senra, F. Vilas-Boas, M. M. Rodrigues, A. C. Campos-de-Carvalho, R. Ribeiro-Dos-Santos, and M. B. Soares.** 2005. Treatment with benznidazole during the chronic phase of experimental Chagas' disease decreases cardiac alterations. Antimicrob. Agents Chemother. **49:**1521–1528.
6. **Garg, N., and R. L. Tarleton.** 2002. Genetic immunization elicits antigen-specific protective immune responses and decreases disease severity in *Trypanosoma cruzi* infection. Infect. Immun. **70:**5547–5555.
7. **Gus, I., M. E. Molon, and A. P. Bueno.** 1993. Chagas disease-review of eight simultaneous cases of acute Chagas myocarditis: 25 years later. Arq. Bras. Cardiol. **60:**99–101.
8. **Hoft, D. F., P. L. Farrar, K. Kratz-Owens, and D. Shaffer.** 1996. Gastric invasion by *Trypanosoma cruzi* and induction of protective mucosal immune responses. Infect. Immun. **64:**3800–3810.
9. **Hoft, D. F., and C. S. Eickhoff.** 2005. Type 1 immunity provides both optimal mucosal and systemic protection against a mucosally invasive, intracellular pathogen. Infect. Immun. **73:**4934–4940.
10. **Hoft, D. F., A. R. Schnapp, C. S. Eickhoff, and S. T. Roodman.** 2000. Involvement of $CD4^+$ Th1 cells in systemic immunity protective against primary and secondary challenges with *Trypanosoma cruzi*. Infect. Immun. **68:**197–204.
11. **Hoft, D. F., R. G. Lynch, and L. V. Kirchhoff.** Unpublished data.
12. **Hoft, D. F., and C. S. Eickhoff.** 2002. Type 1 immunity provides optimal protection against both mucosal and systemic *Trypanosoma cruzi* challenges. Infect. Immun. **70:**6715–6725.
13. **Luhrs, K. A., D. L. Fouts, and J. E. Manning.** 2003. Immunization with recombinant paraflagellar rod protein induces protective immunity against *Trypanosoma cruzi* infection. Vaccine **21:**3058–3069.
14. **Michailowsky, V., K. Luhrs, M. O. Rocha, D. Fouts, R. T. Gazzinelli, and J. E. Manning.** 2003. Humoral and cellular immune responses to *Trypanosoma cruzi*-derived paraflagellar rod proteins in patients with Chagas' disease. Infect. Immun. **71:**3165–3171.
15. **Miles, M. A.** 1972. *Trypanosoma cruzi*-milk transmission of infection and immunity from mother to young. Parasitology **65:**1–9.
16. **Miller, M. J., R. A. Wrightsman, G. A. Stryker, and J. E. Manning.** 1997. Protection of mice against *Trypanosoma cruzi* by immunization with paraflagellar rod proteins requires T cell, but not B cell, function. J. Immunol. **158:**5330–5337.
17. **Neira, I., F. A. Silva, M. Cortez, and N. Yoshida.** 2003. Involvement of *Trypanosoma cruzi* metacyclic trypomastigote surface molecule gp82 in adhesion to gastric mucin and invasion of epithelial cells. Infect. Immun. **71:**557–561.
18. **Pereira-Chioccola, V. L., F. Costa, M. Ribeirao, I. S. Soares, F. Arena, S. Schenkman, and M. M. Rodrigues.** 1999. Comparison of antibody and protective immune responses against *Trypanosoma cruzi* infection elicited by immunization with a parasite antigen delivered as naked DNA or recombinant protein. Parasite Immunol. **21:**103–110.
19. **Prata, A.** 1999. Evolution of the clinical and epidemiological knowledge about Chagas disease 90 years after its discovery. Mem. Inst. Oswaldo Cruz. **94**(Suppl. 1)**:**81–88.
20. **Schijman, A. G., C. A. Vigliano, R. J. Viotti, J. M. Burgos, S. Brandariz, B. E. Lococo, M. I. Leze, H. A. Armenti, and M. J. Levin.** 2004. *Trypanosoma cruzi* DNA in cardiac lesions of Argentinean patients with end-stage chronic Chagas heart disease. Am. J. Trop. Med. Hyg. **70:**210–220.
21. **Schnapp, A. R., C. S. Eickhoff, D. Sizemore, R. Curtiss III, and D. F. Hoft.** 2002. Cruzipain induces both mucosal and systemic protection against *Trypanosoma cruzi* in mice. Infect. Immun. **70:**5065–5074.
22. **Scott, P., E. Pearce, A. W. Cheever, R. L. Coffman, and A. Sher.** 1989. Role of cytokines and $CD4^+$ T-cell subsets in the regulation of parasite immunity and disease. Immunol. Rev. **112:**161–182.
23. **Sepulveda, P., M. Hontebeyrie, P. Liegeard, A. Mascilli, and K. A. Norris.** 2000. DNA-based immunization with *Trypanosoma cruzi* complement regulatory protein elicits complement lytic antibodies and confers protection against *Trypanosoma cruzi* infection. Infect. Immun. **68:**4986–4991.
24. **Shikanai-Yasuda, M. A., C. B. Marcondes, L. A. Guedes, G. S. Sigueira, A. A. Barone, J. C. P. Dias, V. Amato Neto, J. E. Tolezano, B. A. Peres, E. R. Arruda, Jr., M. H. Lopes, M. Shiroma, and E. Chapadeiro.** 1991. Possible oral transmission of acute Chagas' disease in Brazil. Rev. Inst. Med. Trop. Sao Paulo **33:**351–357.
25. **Sibley, L. D., and N. W. Andrews.** 2000. Cell invasion by un-palatable parasites. Traffic **1:**100–106.
26. **Tardieux, I., P. Webster, J. Ravesloot, W. Boron, J. A. Lunn, J. E. Heuser, and N. W. Andrews.** 1992. Lysosome recruitment and fusion are early events required for trypanosome invasion of mammalian cells. Cell **71:**1117–1130.
27. **Vasconcelos, J. R., M. I. Hiyane, C. R. Marinho, C. Claser, A. M. Machado, R. T. Gazzinelli, O. Bruna-Romero, J. M. Alvarez, S. B. Boscardin, and M. M. Rodrigues.** 2004. Protective immunity against *Trypanosoma cruzi* infection in a highly susceptible mouse strain after vaccination with genes encoding the amastigote surface protein-2 and *trans*-sialidase. Hum. Gene Ther. **15:**878–886.
28. **Wizel, B., M. Nunes, and R. L. Tarleton.** 1997. Identification of *Trypanosoma cruzi trans*-sialidase family members as targets of protective $CD8^+$ TC1 responses. J. Immunol. **159:**6120–6130.
29. **Wizel, B., N. Garg, and R. L. Tarleton.** 1998. Vaccination with trypomastigote surface antigen 1-encoding plasmid DNA confers protection against lethal *Trypanosoma cruzi* infection. Infect. Immun. **66:**5073–5081.

Editor: J. F. Urban, Jr.